# Pole-zero Localization: A Behavioral Modeling Approach

Christopher Gathercole
Department of Electrical Engineering
University of Arkansas, Fayetteville 72701
cgather@comp.uark.edu

H. Alan Mantooth
Department of Electrical Engineering
University of Arkansas, Fayetteville 72701
mantooth@engr.uark.edu

***Abstract****-A behavioral modeling procedure has been developed that enables the movement of poles and zeros to be modeled with changes in operating conditions. A major component of this procedure, known as the root localization algorithm, identifies when such an approach is applicable, resulting in models that more accurately reflect the distinctive behavior of the circuit.*

## 1. Introduction

Model order reduction techniques that enable the creation of highly accurate low-order models for linear circuits exist today [1-4]. Often, the roots (*poles and zeros*) of these models do not reflect the actual roots arising in the circuit, and so long as the model characteristics accurately match those of the circuit the model is considered to be accurate. However, such modeling techniques produce models that are accurate for only one operating condition. In [5], a unique step-by-step modeling procedure was described that enables the extraction of nonlinear dynamic behavior (*i.e., pole and zero movement as a function of operating conditions*) when modeling nonlinear circuits.

Using the circuit netlist and specifications this modeling procedure produces differential equation-based behavioral models that, unlike other modeling procedures, can represent pole / zero movement with changing operating conditions, thus improving accuracy and also model efficiency. An integral part of this modeling procedure, and the topic of this paper, is the root localization algorithm. This algorithm utilizes a signal path-tracing algorithm, circuit specifications, and root sensitivity measurements to classify critical nodes in the circuit necessary for creation of bias-sensitive models.

The classifications provided by the root localization algorithm allow the modeler to identify when it is possible to use the bias-sensitive modeling technique described here. The ability to model poles and zeros in this way results in models that are more predictive of the circuit's distinctive (and nonlinear) behavior.

This paper will describe the modeling approach taken when using the root localization in section two; discuss the mathematics of the algorithm in section three; explain in section four the ways in which poles and zeros are implemented in the behavioral model once the algorithm has been employed; and finally illustrate the algorithm through the use of an op-amp example in section five.

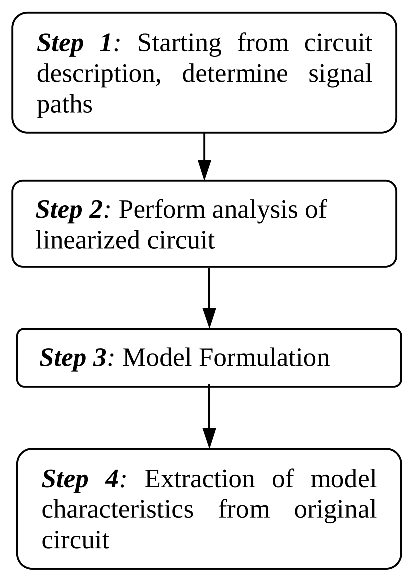


*Figure 1. Bottom-up behavioral modeling procedure.*

## 2. Modeling Approach

To understand the context of the root localization algorithm it is necessary to briefly describe the modeling procedure it is a part of, which is graphically represented by the flowchart in Figure 1 shown above. The first step in the modeling procedure is to classify nodes as signal path nodes or non-signal path nodes. A signal path node is one through which the signal passes in order to go from an input node to an output node. All other nodes are classified as non-signal path nodes. There are usually multiple signal paths in a circuit and the modeler typically possesses such knowledge in advance. However, an automated signal path-tracing algorithm (SPT) exists to aid in the determination.

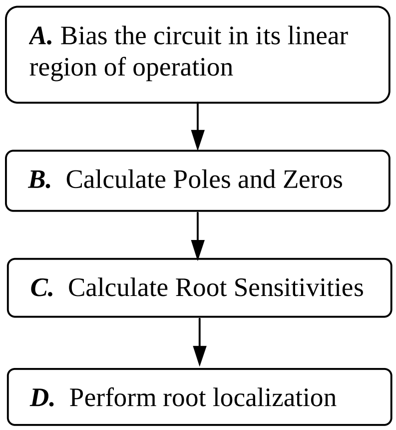


*Figure 2. Analyses performed on linearized circuit.*

The second step in the modeling procedure is to perform a linear analysis of the circuit, which is graphically represented by a flowchart in Figure 2. For this step the circuit must be biased in its linear region of operation such that analysis would consists of only the small-signal models of its components, namely its diodes, BJT's, and MOSFETs. This modeling procedure is only applicable to circuits that can be linearized about an operating point. The high-gain region of an op-amp is an example of such an operating point. Even though the circuit is required to be biased at one operating point, the goal is to produce a model that is valid, or at the very least, informative for multiple operating conditions, as will be discussed later. Once the circuit is biased at what is considered to be normal operating conditions, it is then necessary to determine the poles and zeros and perform root sensitivity analyses, which indicate to what extent a root is sensitive to element value changes. It is at this point where the root localization algorithm is used. In an arbitrary circuit, the poles and zeros will often arise largely due to the reactive elements connected to a single node or between a pair of nodes. The root localization algorithm attempts to determine the degree to which a root in the original circuit can be "localized" to a single node or a coupled pair of nodes. When this occurs, such roots will be referred to as *localized*. In contrast, other poles and zeros are not dominated by elements at a single node, or two, but rather are a function of many elements connected in various parts of the circuit. These roots will be referred to as *delocalized*. The root localization algorithm uses root sensitivity calcualtions to determine the extent to which roots are localized or delocalized. Once this classification has been made, localized and delocalized roots can be further classified as signal path or non-signal path roots. A root may be localized to a certain node, however if it is not in the signal path, it need not be included in the model (*i.e., eliminate bias circuitry-based roots*). The specific details of the algorithm itself will be presented in the next section.

The third step of the modeling procedure is where the model formulation occurs. In this step additional nodes, which may be important topologically, are identified for inclusion in the model and the set of differential algebraic equations that represent the model behavior are derived. An example of important nodes would be nodes where signals are summed from different parts of the circuit.

Finally, the fourth step of the modeling procedure involves the extraction of behavioral model characteristics from the original circuit by obtaining data tables through simulation. This step is used to ensure that the model characteristics match the desired characteristics as closely as possible.

## 3. Algorithm

As mentioned earlier, the root localization algorithm uses root sensitivity calculations to determine the extent to which roots are localized to certain nodes. For every root, a root sensitivity calculation is made with respect to each element *h* using the following normalized expressions for poles and zeros, respectively.

$$S_h^p = \frac{h}{p}\left(\frac{\partial p}{\partial h}\right) \quad \text{and} \quad S_h^z = \frac{h}{z}\left(\frac{\partial z}{\partial h}\right) \qquad (1)$$

Division by the root values in the above expressions indicates that the real and imaginary parts are independently normalized. Thus for a generic root $r_j = \sigma + j\omega$, the root sensitivity is given by

$$S_h^{r_j} = \frac{h}{\sigma}\left(\frac{\partial \sigma}{\partial h}\right) + j\frac{h}{\omega}\left(\frac{\partial \omega}{\partial h}\right). \qquad (2)$$

Even though non-reactive elements contribute to root values, the root localization algorithm does not consider them since experimental results have shown that such sensitivities do not accurately predict localized roots. This is intuitive as inductors and capacitors are the elements that give rise to roots. Furthermore, since inductors are not used on ICs nor found in the small signal models of transistors and diodes, only capacitive elements will be considered from this point. Thus, for a circuit with four roots and four capacitances there will be a total of 16 root sensitivities.

Once the root sensitivities have been calculated, the first step of the root localization algorithm is to calculate the total sensitivity of a root given by the following expression:

$$S_{T,j} = \sum_{i=1}^{n} \left| S_{C_i}^{r_j} \right| \tag{3}$$

where $n$ is the number of capacitors and $j$ is the number of roots. Thus, there will be a total sensitivity calculation for each root in the circuit.

The second step of the algorithm is to calculate the nodal sensitivity ratio (NSR) $M_k$ given by the following expression:

$$M_{k,j} = \frac{\sum_{i=1}^{l_k} \left| S_{C_i}^{r_j} \right|}{S_{T,j}} \quad k = 1, 2, \ldots, m \tag{4}$$

where $m$ is the number of nodes in $N$ and $l_k$ is the number of capacitors connected to the node $k$. Thus, there will be a NSR for each combination of root and node in the circuit. The result $M_{k,j}$ represents the ratio of the sum of the root sensitivities with respect to the capacitances connected to a single node $k$ in the network $N$ to the total sensitivity measure $S_{T,j}$. The ratio portrays what percentage of the overall capacitive sensitivity is due to the capacitances connected to node $k$. Put otherwise, the NSR indicates to what extent a root is localized to a single node.

Two user-specified tolerances are used to determine what extent is acceptable for a root to be considered localized: an absolute tolerance and a relative tolerance. The absolute tolerance is imposed on each NSR and sets the maximum amount of error that is acceptable for a root to be considered localized to the corresponding node. For an absolute tolerance of 0.10, the NSR must be greater than 0.90 (1-0.10) for the corresponding node and root to be considered as a localized pair.

A relative tolerance is also used to ensure that the largest NSR for a root $r_j$ is sufficiently greater than the second largest. If the second largest NSR is sufficiently large, but does not meet the absolute tolerance, it would be incorrect to assume that the root is localized simply because the largest nodal sensitivity ratio meets the absolute tolerance. For example, if the nodal sensitivity ratios $M_{1,j}$ and $M_{2,j}$ of a root $r_j$ are close in value, but $M_{1,j}$ meets the absolute tolerance and $M_{2,j}$ does not, it would be incorrect to claim that the root $r_j$ is localized to node 1 since a significant portion of the root is sensitive to elements connected to node 2. If the relative tolerance were 0.4, $M_{2,j} / M_{1,j}$ must be greater than 0.6 (1 - 0.4) to be localized. It is important to note the tolerances do necessarily mean that the results will be that bad, but rather that the results are guaranteed to be *at least* that good. A NSR of 0.99 would indicate that the pole is highly localized within in 1% regardless of the absolute tolerance.

In the event that none or more than one of the nodal sensitivity ratios for a given root meet the absolute tolerance further analysis is performed to determine if the root is localized to a coupled pair of nodes. To do so, the NSRs are sorted from largest to smallest and a cross nodal sensitivity ratio (CNSR) is calculated using the following expression:

$$M_{xy,j} = M_{x,j} + M_{y,j} - \frac{\sum_{i=1}^{lxy} \left| S_{C_i}^{r_j} \right|}{S_T} \tag{5}$$

where $M_{x,j}$ is the largest NSR and $M_{y,j}$ is the next largest sensitivity ratio in which the corresponding node $y$ is capacitively coupled to node $x$ of the largest NSR. The last term represents the common factors in $M_{x,j}$ and $M_{y,j}$ due to the coupling capacitances between nodes $x$ and $y$ which must be subtracted to avoid redundancy.

After the largest NSR $M_{x,j}$ and the next largest coupled NSR $M_{y,j}$ are used to calculate $M_{xy,j}$ the algorithm moves the third largest coupled NSR $M_{z,j}$ which is used to calculate another CNSR $M_{xz,j}$. Once all the NSRs whose corresponding nodes are capacitively coupled to the largest NSR $M_{x,j}$ have been used to calculate a set of CNSRs, the algorithm is repeated using the second largest NSR as $M_{x,j}$ and the process repeats using only NSRs smaller than the new $M_{x,j}$, thus avoiding redundant CNSR calculations.

The results of the CNSR calculations are interpreted just as the original NSRs were (*using absolute and relative tolerances*) to determine if a root is localized to a capacitively coupled pair of nodes. If no or multiple CNSRs meet the tolerance requirements then the node is classified as delocalized.

The root localization algorithm is applied to every root after its calculation from the linearized circuit. The roots are divided into two groups as a result of the application of the algorithm: localized and delocalized. The localized roots are then divided into signal and non-signal path roots based on their nodal correspondence. The delocalized roots are further analyzed to determine whether or not they influence the signal from input to output by summing the largest NSRs until the tolerance is met and then determining if any NSRs included in the summation correspond to those of signal path nodes. Only one signal path node is required to make a delocalized root a signal path root, thus worthy of consideration for inclusion in the behavioral model.

## 4. Implementation

The classifications provided by the root localization algorithm allow the modeler to begin developing the behavioral model of the circuit. The first step in this process is it to eliminate any roots that do not fall in the frequency range over which the models are required to be accurate. For op-amps and comparators a good convention is to include only those poles and zeros that fall within a decade beyond the gain bandwidth.

Next, the modeler must choose to model the roots in one of two ways: *physically* or *linearly*. The term “physically” is used to mean that the nonlinear static and the linear dynamic characteristics of the root are accurately modeled such that the model is valid for all domains of simulation. A root can be modeled physically when it is localized to a node in the circuit. A general representation of a physically modeled node is given below in Figure 3.

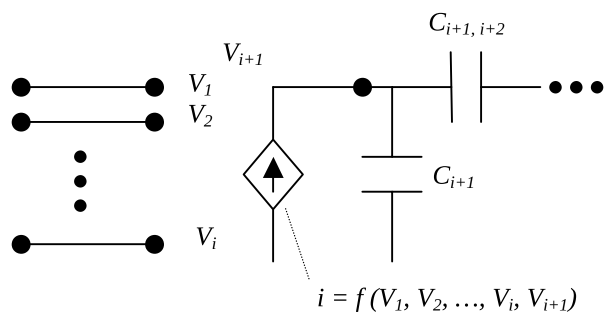


*Figure 3. General representation of a physically modeled node.*

Notice that the controlled current source in Figure 3 is not only a function of node voltages elsewhere in the circuit, but also the voltage of the node to which it is connected. In this way a nonlinear resistance is incorporated as part of the source, since the current into the node partially depends on its voltage. The nonlinear resistance of the current source and the capacitances connected at the node determine the root value. Other commonly used modeling techniques use both constant resistances and capacitances to model root values. In this way, the roots are not sensitive to other parts of the circuit and thus are not sensitive to changes in operating conditions. The method described here, models roots in such a way that they are sensitive to other parts of the circuit resulting in models that are valid for all domains of simulation. Signal path nodes that have localized roots are examples of those that will be modeled physically. Non-signal path nodes that do not have localized roots can be excluded from the model since they do not affect the signal from input to output (*i.e., eliminate bias circuitry-based roots*).

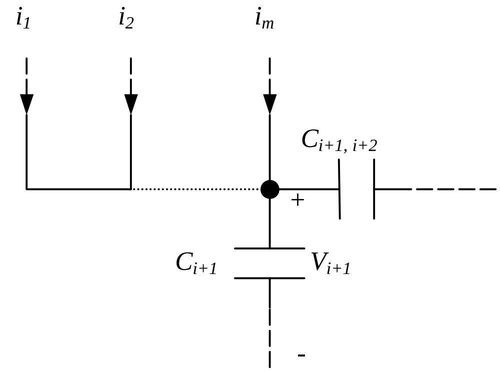


*Figure 4. General node in an analog circuit.*

A general nonlinear ordinary differential equation can be derived to model a node physically from Figure 4, which depicts a general node in an analog circuit. From this figure the following nonlinear ordinary differential equation can be written.

$$i_1 + i_2 + \cdots + i_m + C_{eq}\frac{dV_{i+1}}{dt} - \sum_{j=1}^{n} C_{i+1,j}\frac{dV_j}{dt} = 0 \quad (6)$$

or

$$\sum_{k=1}^{m} i_k + C_{eq}\frac{dV_{i+1}}{dt} - \sum_{j=1}^{n} C_{i+1,j}\frac{dV_j}{dt} = 0 \quad (7)$$

where $i_1$, $i_2$, …, $i_m$ are the current contributions to the $i+1^{st}$ node (via transistors, resistors, diodes, etc.) and

$$C_{eq} = C_{i+1} + \sum_{j=1}^{n} C_{i+1,j}\ . \quad (8)$$

$C_{i+1,\ j}$ are the coupling capacitances between node $i+1$ and other nodes. By letting

$$i_s = -\sum_{k=1}^{m} i_k \quad (9)$$

the nonlinear differential equation above can be rewritten as

$$i_s = C_{i+1}\frac{dV_{i+1}}{dt} + C_{i+1,i+2}\frac{d(V_{i+1} - V_{i+2})}{dt} \quad (10)$$

to correspond to the equation of the general physically modeled node given in Figure 3, where only one coupling capacitance has been used for simplicity.

Once a root has been determined to be localized to a single node, the nonlinear dc forcing function and nonlinear resistance at the node must be extracted from the original circuit by extracting a data table through transistor level simulation. These tables are determined by tabulating currents as a function of voltages throughout the circuit, whose relationships can be determined from the signal path analysis. As described above, since the current into the node in Figure 3 depends partially upon its voltage, these current-voltage relationships can be thought of as source currents and nonlinear resistances in tandem. Thus, once the table extraction is complete, the resistance value at the operating point from which the circuit was linearized can be determined. Using this resistance value and the pole value, the equivalent capacitance for the model can be determined. For an in depth description of the equations used to determine the equivalent capacitance for either a single node or a coupled pair of nodes refer to Appendix A in [6].

The other way in which a root can be modeled is linearly. To model a root linearly simply involves implementing a transfer function. The differential equations describing these roots will be linear and are not intimately associated with the nonlinearities present in the actual circuit. The modeler can choose to model a localized pole using linear or nonlinear differential equations depending on the importance of the static nonlinearities at the node. However, a delocalized root must be modeled linearly. Thus, roots that are determined to be delocalized will be modeled using a transfer function comprised of these poles and zeros.

## 5. Operational Amplifier Example

The following example will be used to illustrate the way in which the root localization algorithm is used to aid in the development of behavioral models. Figure 5 is the schematic of a high dynamic-range CMOS op-amp. Details about this circuit can be found in [7]. As can be seen from the schematic, it consists of two differential amplifiers and a completely symmetrical output structure intended to reduce distortion.

As outlined earlier, the first step in the modeling process is to determine the signal path nodes of the circuit. They are nodes 1, 2, 3, 4, 5, 6, 7, 8, 12, 13, 20, and 22. The second step is to determine the operating point about which the circuit is to be linearized. For an op-amp, the natural selection is to bias it in the high-gain linear region of operation. Thus, the inputs should be set at the mid-supply voltage with an input referred –8.44 mV on the noninverting terminal to compensate for the systematic offset voltage. Once the circuit has been linearized about an operating point, the next step is to determine the poles and zeros in the circuit. The results are given in Table 1.

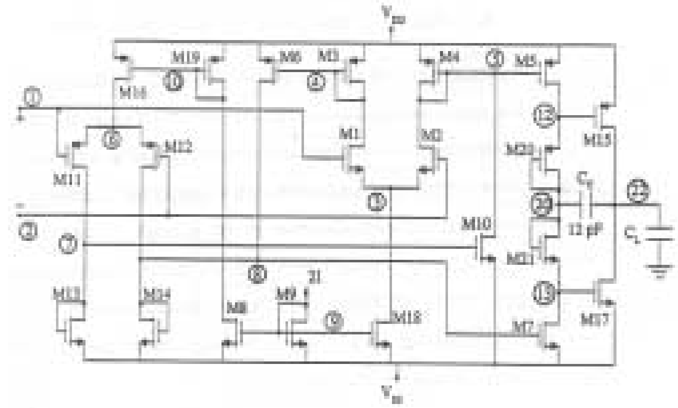


Figure 5. High Dynamic-range Op-amp

**Table 1. Differential-mode Pole-zero Analysis of Op-amp**

| | Poles (kHZ) | | | Zeros (kHz) | |
|---|---|---|---|---|---|
| j | Real | Imag. | j | Real | Imag. |
| 1 | -.029 | 0 | 13 | -199 | 22 |
| 2 | -107 | 0 | 14 | -199 | -22 |
| 3 | -162 | 0 | 15 | -307 | 0 |
| 4 | -381 | 0 | 16 | -808 | 402 |
| 5 | -459 | 0 | 17 | -808 | -402 |
| 6 | -745 | 0 | 18 | -1,196 | 645 |
| 7 | -793 | 0 | 19 | -1,196 | -645 |
| 8 | -1,346 | 0 | 20 | -1,626 | 0 |
| 9 | -1,601 | 0 | 21 | -2403 | 0 |
| 10 | -1,636 | 0 | | | |
| 11 | -2,404 | 0 | | | |
| 12 | -4,271 | 0 | | | |

The gain-bandwidth of the op-amp was determined to be approximately 100 kHz by transistor level simulation. Any roots not within one decade past the bandwidth were eliminated for consideration of inclusion in the model. The shaded boxes represent those roots that meet this criterion.

At this point the root localization algorithm is used and the nodal sensitivity ratios (NSRs) are calculated. Using an absolute tolerance of 10% and a relative tolerance of 40% it was determined that four poles and one zero are localized. The nodal sensitivity ratios for the poles and zeros are shown below in Table 2.

Inspection of the Table 2 reveals that for three roots a single nodal sensitivity ratio (NSR) stands out as being much larger than all others. These roots are indicated in columns where only one is box is shaded. A value of 1 for $M_{4,2}$ reveals that the pole at 107 kHz arises solely due the capacitances connected at node four. Thus, modeling node four physically is all that is required to model this pole and the equation would take on the form of eq. 10. The same situation exists for the pole at 460 kHz and node 5. The result of 0.939 for $M_{22, 3}$ reveals that the pole at 162 kHz is localized to node 22, but not as exclusively as the poles at 107 kHz and 460 kHz were localized to their corresponding nodes. For these two highly localized roots, one notices that the nodal sensitivity ratios in the respective columns are very small percentages—much less than 1%. For the pole at 162 kHz this is not the case, since there is an approximate nodal sensitivity ratio of 12% corresponding to node 20. The root still arises mostly due to the capacitances connected to node 22, however it can be seen that the process is interpretive.

**Table2. Nodal Sensitivity Ratios of Localized Poles and Zeros**

| | | Poles (kHz) | | | Zero (kHz) |
|---|---|---|---|---|---|
| | -0.029 | -107 | -162 | -460 | -307 |
| | $M_{k, 1}$ | $M_{k, 2}$ | $M_{k, 3}$ | $M_{k, 5}$ | $M_{k, 15}$ |
| $M_{1, j}$ | 20.3 f | .216 m | 45.1 n | .142 m | 32.4 µ |
| $M_{2, j}$ | .283 p | 41.8 µ | .100 µ | .483 m | 21.7 µ |
| $M_{3, j}$ | 17.4 f | .103 m | 68.1 µ | .338 m | 34.4 µ |
| $M_{4, j}$ | 2.80 p | 1 | 1.45 µ | 8.70 µ | .281 m |
| $M_{5, j}$ | 12.7 µ | 2.96 µ | .472 m | 0.997 | .693 m |
| $M_{6, j}$ | 31.0 f | 1.06 µ | 44.1 n | 62.5 µ | 33.7 µ |
| $M_{7, j}$ | .426 p | .403 µ | .123 µ | 1.08 m | 72.0 µ |
| $M_{8 j}$ | 5.76 µ | 1.27 m | .117 µ | 35.3 µ | 79.8 µ |
| $M_{9, j}$ | 8.93 a | 1.26 µ | 1.36 n | .363 m | 70.4 µ |
| $M_{10 ,j}$ | 60.6 a | 3.64 n | .131 n | 71.1 µ | 35.2 µ |
| $M_{12, j}$ | 2.17 m | .579 µ | 34.7 m | 3.8 m | 46.8 m |
| $M_{13, j}$ | .811 m | .189 µ | 10.3 µ | 12.2 µ | 3.00 m |
| $M_{20, j}$ | 0.989 | 1.15 µ | 0.119 | 1.06 m | 0.998 |
| $M_{22, j}$ | 0.997 | 3.11 µ | 0.939 | 1.18 m | 0.922 |

Further inspection of Table 2 reveals that for two roots, one NSR did not stand out: they are the dominant pole at 29 Hz and the zero at 307 kHz. For these roots, two NSRs meet the tolerance of 10%. Therefore, in each case a cross nodal sensitivity ratio (CNSR) must be further calculated to determine if the root is localized. Using $M_{20, 1}$ and $M_{22, 1}$ as $M_{x, j}$ and $M_{y, j}$, respectively, the resulting CNSR was calculated to be 0.998 for the dominant pole at 29 Hz. Thus this pole is highly localized to the coupled nodes 20 and 22, which is expected since inspection of the op-amp schematic in Figure 5 reveals that the Miller capacitance is connected between these two nodes. Similarly, using $M_{20, 15}$ and $M_{22, 15}$ for the zero at 307 kHz resulted in a CNSR of 0.998 as well. Thus, both the zero and dominant pole are localized to the capacitively coupled nodes 20 and 22.

## 6. Conclusion

Most modeling techniques model poles and zeros using linear ordinary differential equations and although they often produce accurate low-order models by simply modeling poles and zeros as a transfer function they sacrifice the ability to model nonlinear dynamic behavior. The root localization provides the modeler with the ability to decide when modeling pole and zero movement is possible through the modeling procedure outlined above. Models created in this fashion are more predictive of the circuit's distinctive behavior while maintaining a high level of accuracy.

As illustrated by the op-amp example in the previous section, the root localization algorithm identifies important nodes in the circuit, which when modeled physically capture the behavior of the localized roots. It is reasonable to conclude that, for models produced in this fashion to be effective, the dominant pole must be localized. When it is, extraneous nodes are eliminated from inclusion in the model and nonlinear dynamic behavior is extracted.

The following plots were obtained from simulation of the resulting op-amp model. As can be seen, the characteristics of the model, represented by the dotted lines, accurately match those of the circuit, represented by the solid lines.

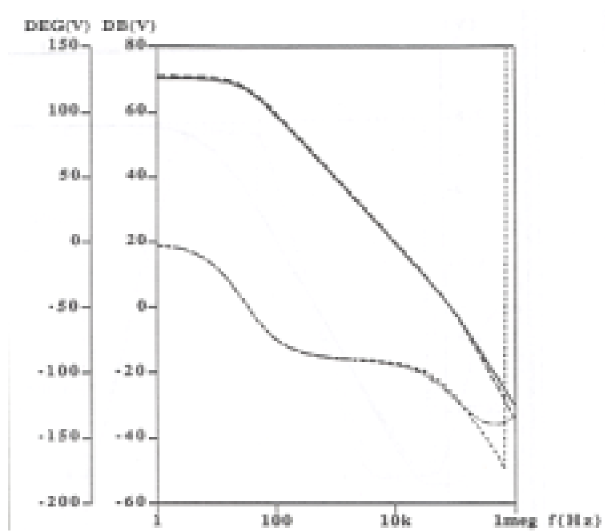


*Figure 6. Frequency response curves (magnitude and phase) of the op-amp and its behavioral model.*

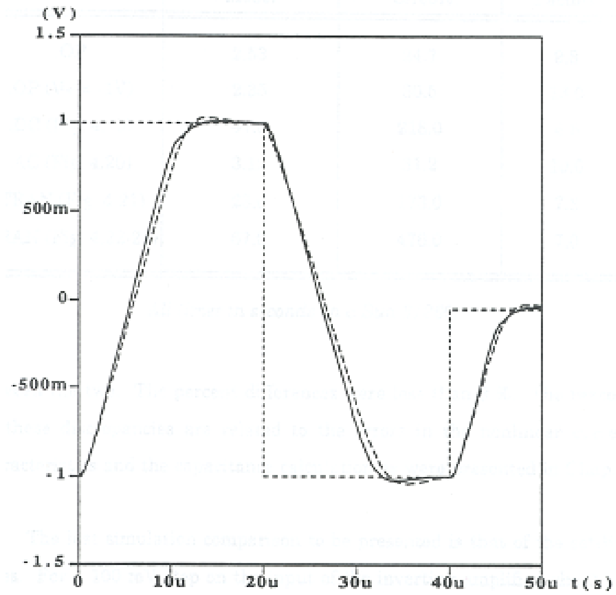


*Figure 7. Large-signal transient response of the op-amp and its behavioral model in a voltage follower configuration.*

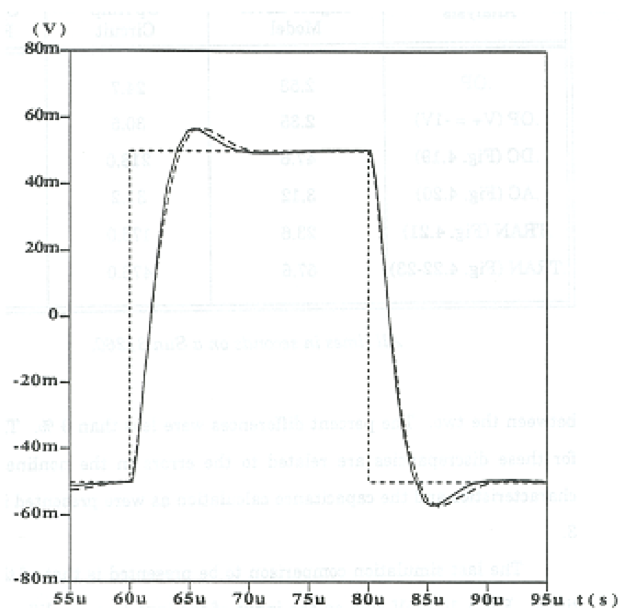


*Figure 8. Small-signal transient response of the op-amp and its behavioral model in a voltage follower configuration.*

## References


[1] Eli Chiprout and Michel S. Nakhla, *Asymbolic Waveform Evaluation and Moment Matching for Interconnect Analysis*, Kluwer Academic Publishers, 1994.

[2] A. Odabasioglu, M. Celik, and L.T. Pileggi, “Practical considerations for passive reduction of RLC circuits.” *IEEE/ACM 1999 International Conference on Computer-Aided Design*. pp. 214 – 219, 1999.

[3] J. Roychowdhury, “Reduced-order modeling of time-varying systems.”, *IEEE Transactions on Circuits and Systems II: Analog and Digital Signal Processing*, vol. 46, no. 10, pp. 1273 –1288, Oct. 1999.

[4] J.-R. Li and J. White, “Efficient model reduction of interconnect via approximate system gramians”, *1999 IEEE/ACM International Conference on Computer-Aided Design*, pp. 380 –383, 1999.

[5] H. A. Mantooth, P. E. Allen, “A higher level modeling procedure for analog integrated circuits,” *International Journal on Analog Integrated Circuits and Signal Processing*, vol. 3, pp. 181-195, May 1993.

[6] H. A. Mantooth, “Higher level modeling of analog integrated circuits,” Ph.D. Dissertation, Georgia Institute of Technology, 175 pp., Sept. 1990.

[7] M. Steyaert and W. Sansen, “A high-dynamic-range CMOS op amp with low distortion output structure,” *IEEE J. Solid-State Circuits*, vol. SC-22, pp. 1204-1207, Dec. 1987.